molecular pharmaceutics

Article

pubs.acs.org/molecularpharmaceutics

# Brain-Specific Delivery of Dopamine Mediated by *N,N*-Dimethyl Amino Group for the Treatment of Parkinson's Disease

Yanping Li, Yangyang Zhou, Bowen Qi, Tao Gong, Xun Sun, Yao Fu, and Zhirong Zhang*

Key Laboratory of Drug Targeting and Drug Delivery Systems, Ministry of Education, Sichuan University, Sichuan, People's Republic of China

Supporting Information

**ABSTRACT:** Parkinson's disease (PD) has become one of the most deadly diseases due to a lack of effective treatment. Herein, *N*-3,4-bis(pivaloyloxy)-dopamine-3-(dimethylamino)propanamide (PDDP), a brain-specific derivative of dopamine, was designed and synthesized, which consists of a brain targeted ligand, *N,N*-dimethyl amino group, and two dipivaloyloxy groups for lipophilic modification. PDDP was investigated both *in vitro* and *in vivo* by comparing with L-DOPA and another derivative (BPD) without *N,N*-dimethyl amino group. PDDP showed a more pronounced accumulation in mouse brain microvascular endothelial cells (bEnd.3) than BPD via an active transport process. The increased cellular uptake of PDDP was proven to be mediated by putative pyrilamine cationic transporters. Following intravenous administration, the concentration of PDDP in the brain was 269.28-fold and 6.41-fold higher than that of L-DOPA and BPD at 5 min, respectively. Additionally, PDDP effectively attenuated the striatum lesion caused by 6-hydroxydopamine (6-OHDA) in rats. More importantly, PDDP presented antioxidant and antiapoptotic effects on 6-OHDA-induced toxicity in human neuroblastoma cells (SH-SY5Y). Thus, *N,N*-dimethyl amino group-based PDDP represents an effective and safe treatment for PD.

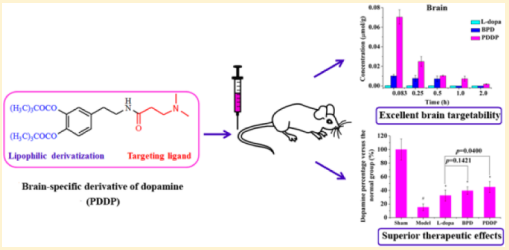


**KEYWORDS:** *N,N-dimethyl amino group, lipophilic derivatization, dopamine, brain-targeting, Parkinson's disease*

## 1. INTRODUCTION

Parkinson's disease (PD) is a progressive neurodegenerative disorder associated with the loss of dopamine (DA) neurons in the nigrostriatal pathway.[1] A population of approximately 5 million globally suffer from PD, and the prevalence is expected to increase dramatically in the coming decades due to the rapid aging of the population worldwide.[2] To date, oral administration of L-DOPA has been the gold standard for PD treatment which compensates for the dopamine deficiency.[3−5] However, L-DOPA therapy is associated with a number of problems such as poor bioavailability and peripheral effects.[6,7] Therefore, developing brain-targeted drug delivery systems would be of great significance to improve the therapeutic effects and reduce the side effects.

The blood brain barrier (BBB), which is characterized by tight junctions between endothelial cells, the absence of fenestrations, and low occurrence of pinocytic activity, presents the greatest challenge for brain drug delivery.[8] To improve the brain penetration, numerous medicinal chemistry- and pharmaceutical technology-based strategies have been explored and developed.[9] Among them, drug-carrier conjugates that can be specifically transported across the BBB via carrier-mediated mechanisms have drawn attention. Recently, glucose transporters (GluT1),[10−12] amino acid transporters (large neutral amino acid transporters 1, LAT1),[13] and 2-phenyl- imidazopyridine moiety-[14] based delivery systems have been successfully developed to specifically deliver L-DOPA or dopamine to the brain. The above conjugates were shown to increase the brain distribution of the parent drug, but no systematic investigation was conducted to address the therapeutic effect and side effects.

In previous works, *N,N*-dimethyl amino group-related structures were proven to significantly enhance the brain-uptake efficiency of dexibuprofen[15] and naproxen.[16] This small molecular ligand offers several advantages for drug development. Specifically, *N,N*-dimethyl amino group possesses a simple and well-defined structure. Moreover, the *N,N*-dimethyl amino group has a high degree of safety without the potential toxicity associated with macromolecular carriers. Additionally, *N,N*-dimethyl amino group has high efficiency of brain targeting which would likely result in superior therapeutic effect. To our best knowledge, no published reports are available regarding *N,N*-dimethyl amino group as a brain-targeted ligand by other groups.

Therefore, *N*-(3,4-dihydroxyphenethyl)-3-(dimethylamino) propanamide (DDP) was initially designed and synthesized, which is the conjugate of dopamine and *N,N*-dimethylamino propanoic acid to improve the brain targetability of dopamine. However, DDP, which could not be transported across the BBB (data not shown), was shown not to be a suitable candidate for brain targeting. Similar results were obtained with other drugs (e.g., zidovudine) conjugated with the *N,N*-dimethyl amino

**Received:** May 13, 2014
**Revised:** June 23, 2014
**Accepted:** July 29, 2014
**Published:** July 29, 2014

**Scheme 1. Synthetic Route of Compounds 3 and 4**[a]

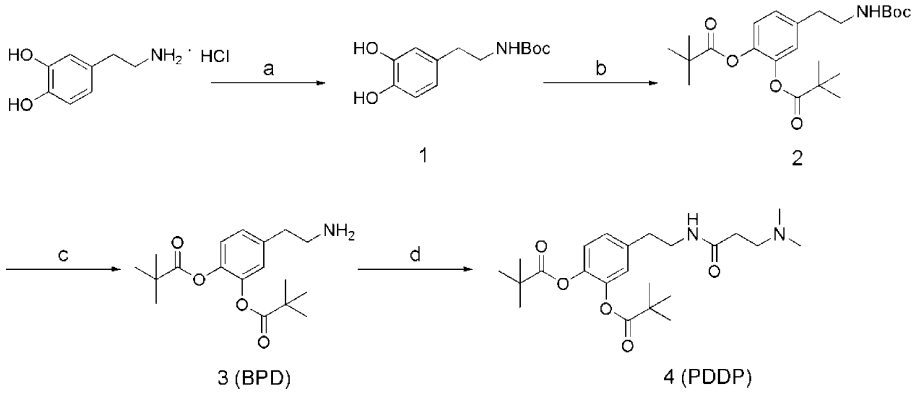


[a]Reagents and conditions: (a) $(Boc)_2$ in dioxane/NaOH aqueous solution; (b) pivaloyl chloride, THF; (c) $CF_3COOH$, $CH_2Cl_2$; (d) 3-(dimethylamino)propanoic acid hydrochloride, EDCI/HOBt, $EtN_3$ in dry $CH_2Cl_2$.

group, which suggested that simply conjugating the drug with the ligand did not result in improved brain targetability of the conjugate. Regarding the differences in physicochemical properties between the two kinds of drugs, nonsteroidal anti-inflammatory drugs (NSAIDs) are lipophilic drugs that have great affinity to tissues. In contrast, dopamine and zidovudine are water-soluble drugs that are easily ionized in the bloodstream and rapidly metabolized.[17] Thus, lipophilicity would be an important impact factor for achieving brain targeting. Therefore, *N,N*-dimethylamino group-conjugated drug derivatives with sufficient lipophilicity appear to be transported more specifically to the brain.

On the basis of this hypothesis, we presented a first attempt to confirm the brain targetability of the *N,N*-dimethyl amino group with improved lipophilicity. Initially, dipivaloyloxy was introduced in the design of the conjugate to achieve the lipophilic derivatization of the catechol system in dopamine. *N*-3,4-Bis(pivaloyloxy)dopamine-3-(dimethylamino)propanamide (PDDP) was thus synthesized and investigated *in vitro* and *in vivo*. Moreover, PDDP showed enhanced cellular uptake in bEnd.3 cells which was attributed to putative pyrilamine cationic transporters. In addition, tissue distribution, brain bioavailability, and therapeutic efficacy of PDDP were evaluated and compared with those of L-DOPA which demonstrated that PDDP would be an excellent candidate to achieve brain-specific dug delivery.

## 2. MATERIALS AND METHODS

**2.1. Materials and Animals.** Dopamine hydrochloride was purchased from Aladdin Chemistry Co. Ltd. (Shanghai, China), L-DOPA and 6-OHDA were supplied by Sigma-Aldrich (St. Louis, MO, U.S.A.) with purity of 99.0%, and 3-(dimethylamino)propanoic acid hydrochloride was obtained from Tokyo Chemical Industry CO. Ltd. (Tokyo, Japan). Annexin V-FITC/PI apoptosis detection kit was purchased from KeyGEN Biotech (China). Acetonitrile (HPLC grade) was purchased from Kemiou (Tianjin, China). All the other chemicals and reagents were of analytical grade obtained commercially.

Sprague−Dawley rats (male; body weight: 200 ± 20 g), provided by the West China Experimental Animal Center of Sichuan University (China), were maintained in a germ-free environment and allowed free access to food and water. All animal experiments were performed in accordance with the principles of care and use of laboratory animals and were approved by the experiment animal administration committee of Sichuan University.

**2.2. Cell Lines and Cell Culture.** L929 (fibroblast cells), bEnd.3 cells (immortalized mouse brain microvascular endothelial cells), and SH-SY5Y (human neuroblastoma cells) were purchased from the American Type Culture Collection (Rockville, MD, U.S.A.) which are from passage 3 to 20. Cells were cultured in DMEM with high glucose (Hyclone, U.S.A.) supplemented with 10% FBS (Hyclone, U.S.A.), 100 IU/mL penicillin, and 100 μg/mL streptomycin. Cells were maintained at 37 °C in a humidified atmosphere containing 5% $CO_2$, and the culture medium was changed every other day.

**2.3. Synthesis and Characterization of *N*-3,4-Bis-(pivaloyloxy)dopamine-3-(dimethyl amino)-propanamide (PDDP).** The synthetic routes of BPD, PDDP, and DDP are described in Scheme 1 and Scheme S1 of the Supporting Information (SI). The detailed methods are presented in the SI.

The stability of BPD and PDDP were investigated in PBS (pH 7.4), plasma, and brain homogenate at 37 °C for 8 h. At predetermined time points, 100 μL of the sample was collected. Then the samples were diluted with acetonitrile, and the percentages of the residual BPD and PDDP were determined by LC−MS/MS.

**2.4. Sample Preparation and LC−MS/MS Analysis.** BPD and PDDP were subjected to hydrolysis before LC−MS/MS analysis. To cell digests (0.1 mL), plasma (0.1 mL), or tissue homogenates (0.1 mL) was added 100 μL pig liver esterase (100 units/mL, Sigma-Aldrich, U.S.A.) and then mixed. After 15 min hydrolysis at 37 °C, dopamine and DDP were released from PD and PDDP, respectively, and 0.6 mL acetonitrile was added. For L-DOPA, 0.2 or 1.0 mL of acetonitrile was added to cell digests (0.1 mL), plasma (0.5 mL), or tissue homogenates (0.5 mL), respectively. The mixtures were vortexed for 5 min and centrifuged at 12,000 rpm for 10 min, and then supernatants (1 μL) were analyzed by LC−MS/MS assay.

The LC−MS/MS system consisted of an Agilent 1200 series RRLC system, which includes an SL autosampler, degasser and SL binary pump, and an Agilent triple-quadruple MS. LC−MS/MS analyses were performed on a diamonsil ODS column (50 mm × 4.6 mm, 1.8 μm) with the corresponding guard column (ODS, 5 μm). The mobile phase consisted of 80% aqueous


dx.doi.org/10.1021/mp500352p | *Mol. Pharmaceutics* 2014, 11, 3174−3185

solution containing 0.1% formic acid and 20% acetonitrile (v/v), at a flow rate of 0.3 mL/min.

Detection was operated on a mass spectrometer in the positive electrospray source ion mode, and quantification was performed using multiple reaction monitoring (MRM). MRM of $m/z$ 154 → 137.1 and 253 → 58.1 were adopted to qualify dopamine and DDP. L-DOPA was monitored at $m/z$ 198.1 → 152. The corresponding optimized collision-induced dissociation voltages of the analysis were 103 and 20 eV for the fragmentor and collision energy, respectively. Instrumental parameters were as follows: gas temperature of 350 °C, gas flow of 8 mL/min, nebulizer of 30 psi, capillary of 4000 v.

**2.5. Cellular Uptake Assay.** *2.5.1. Time-Dependent Cellular Uptake.* The bEnd.3 cells were seeded in 6-well culture plates ($5 \times 10^5$ cells/well). On the second day, when they had grown to confluence, cells were exposed to L-DOPA, BPD, and PDDP, which were diluted in Hank's buffer (122 mM NaCl, 3 mM KCl, 25 mM $NaHCO_3$, 1.2 mM $MgSO_4$, 1.4 mM $CaCl_2$,10 mM D-glucose, 10 mM HEPES, pH 7.4) at a final concentration of 40 $\mu$M. Then bEnd.3 cells were incubated in triplicate for 0.25, 0.5, 1, or 2 h, respectively. After that, cells were washed with PBS (pH 7.4) to remove extracellular drugs. Cells were then trypsinized, centrifuged at 3000 rpm for 5 min, and cell pellets were washed twice with PBS. The cell pellets were added with ultrapure water and lysed by repetitive freeze−thawing to release the intracellular drugs. Sample processing procedures are described in section 2.4, and the intracellular concentrations of L-DOPA, BPD, or PDDP were measured by LC−MS/MS. Cellular uptake was expressed as the amount (nmol) of L-DOPA, BPD, or PDDP per 1 mg of total cellular protein. The total protein of cell lysates was determined in parallel wells by BCA assay (Pierce, U.S.A.).

*2.5.2. Dose-Dependent Cellular Uptake.* The bEnd.3 cells were seeded in 6-well culture plates ($5 \times 10^5$ cells/well). On the second day, cells were incubated with L-DOPA, BPD, or PDDP at the following concentrations, 10, 20, 40, and 80 $\mu$M, respectively, for 0.5 h at 37 °C. Cells were rinsed three times with ice-cold PBS and collected for the determination of intracellular concentration.

*2.5.3. Effect of Temperature and Energy Inhibitors on Cellular Uptake.* The bEnd.3 cells were seeded in 6-well culture plates ($5 \times 10^5$ cells/well). On the second day, cells were exposed to L-DOPA, BPD or PDDP (40 $\mu$M) for 0.5 h at 37 °C, 4 °C, or in the presence of $NaN_3$. Then, cells were washed three times with ice-cold PBS and collected for the determination of intracellular concentration.

*2.5.4. Cellular Uptake on Different Cell Lines.* The bEnd.3 cells and L929 cells were incubated with L-DOPA, BPD or PDDP (40 $\mu$M) for 0.5 h at 37 °C, respectively. Then, cells were washed three times with ice-cold PBS and collected for the determination of intracellular concentration.

**2.6. Mechanistic Study in the Brain Uptake of PDDP *in vitro*.** *2.6.1. Competitive Inhibition Assay.* The bEnd.3 cells were incubated with Hank's buffer in the absence or presence of various inhibitors. After incubation for 15 min at 37 °C, PDDP (40 $\mu$M) was added to the cells, and then the mixture was incubated for another 0.5 h. Then cells were rinsed three times with ice-cold PBS and collected as the sample for each group. The intracellular concentration of PDDP was determined as described before.

*2.6.2. The Uptake Property of PDDP in bEnd.3 Cells.* In sodium-free experiments, sodium ions were replaced with *N*-methylglucamine or potassium chloride. For the study of valinomycin, a potassium ionophore, cells were preincubated with 10 $\mu$M valinomycin for 10 min, and then uptake of PDDP was measured as described above. The uptake was also measured at acidic or alkaline pH (6.0 and 8.4, respectively).

**2.7. Tissue Distribution and Brain Bioavailability in Rats.** L-DOPA, BPD, or PDDP were injected through tail vein of the rats. For each preparation and sampling time point, five rats were treated with a single dose of L-DOPA, BPD, and PDDP which was 19.31, 31.43, and 41.17 mg/kg respectively, equivalent to 18 mg/kg dopamine. The rats were sacrificed at 5, 15, 30, 60, and 120 min after injection. The blood plasma and tissue homogenates (hearts, livers, spleens, lungs, kidneys, and brains) were quickly collected and stored at −40 °C until assay.

For the brain bioavailability study, the experimental procedures were kept similar to the biodistribution study. At each predetermined time point, rats were sacrificed, and brains were quickly collected and stored at −40 °C until assay. Tissue concentration of drug was measured accordingly.

**2.8. Therapeutic Effect on 6-OHDA-Induced PD Rat Model.** *2.8.1. Unilateral Intrastriatal Infusion of 6-OHDA.* 6-OHDA-induced PD rat model was established according to K. Hu et al.[18] Male Sprague-Dawley (SD) rats (250 ± 20 g) were anesthetized with chloral hydrate (400 mg/kg, *i.p.*), and then placed in a stereotaxic apparatus (Anhui Zhenghua Bio Equipment Co., Ltd., Huaibei, China) to achieve a flat skull position. A sagittal incision was made in the scalp with sterile blade, then the skin and inferior tissue layers covering the skull were retracted and a small hole was drilled at the following coordinates: lateral (L) 3 mm, antero-posterior (AP) 0.2 mm, dorso−ventral 4.8, and 5.6 mm from the bregma point. The 6-OHDA solution (10 $\mu$g/mL dissolved in 0.2% ascorbic acid) was infused unilaterally through a stainless steel cannula into the striatal region at 0.3 $\mu$L/min, 1 $\mu$L each point. Another group of rats, which were injected with a 6-OHDA-free solution (0.2% ascorbic acid saline) in a similar manner, served as the sham group.

*2.8.2. Experimental Design.* Sixty rats were randomly divided into the following five groups ($n$ = 12). Sham-operated group: rats were subjected to the surgical procedure as described above; 6-OHDA lesioned group: in this group, rats were injected with normal saline via caudal vein every day after 6-OHDA lesioning; 6-OHDA + L-DOPA group: rats received L-DOPA (5 mg/kg/day) via caudal vein every day after 6-OHDA lesioning; 6-OHDA + BPD group: rats received BPD (8.15 mg/kg/day, equal to 5 mg/kg/day of L-DOPA) via caudal vein every day after 6-OHDA lesioning; 6-OHDA + PDDP group: Rats received PDDP (10.66 mg/kg/day, equal to 5 mg/kg/day of L-DOPA) via caudal vein every day after 6-OHDA lesioning. After 21 days, all rats were sacrificed, and brains were harvested for immunohistochemistry stain of tyrosine hydroxylase (TH), LC−MS/MS detection of the dopamine, and assessment of enzymatic antioxidants.

*2.8.3. Detection of Striatal Dopamine.* Five rats of each group were sacrificed with each left and right striatum harvested separately for the detection of dopamine (DA) as described previously. Briefly, each striatum was sonicated in 0.1 M perchloric acid, and then diluted with acetonitrile. Homogenates were vortexed for 5 min and centrifuged at 12,000 rpm for 10 min at 4 °C. The supernatants were collected and detected with LC−MS/MS method as described above.

*2.8.4. Tyrosine Hydroxylase (TH) Immunohistochemistry.* Two rats of each group were anaesthetized with chloral hydrate, and perfused with normal saline and followed by 4%

paraformaldehyde in PBS. The brains were removed, kept in 4% paraformaldehyde fixative overnight and embedded in paraffin and serially cut for TH immunohistochemistry according to previous studies.[18,19] Photomicrographs were taken with a microscope camera (Nikon Eclipse 80i, Nikon Instech Co. Ltd., Kawasaki, Kanagawa, Japan) at 50× magnification.

*2.8.5. Studies Related to Oxidative Stress.* To assess free radical-mediated effects following 6-OHDA lesioning and to explore the free radical scavenging potential of PDDP, reduced glutathione (GSH), enzymatic antioxidants (total superoxide dismutase and catalase), and total antioxidant capacity (T-AOC) were estimated in the striatum. Five rats from each group were sacrificed, and their brains were dissected quickly on ice pack. Ipsilateral striatum was separated, weighed, and freshly processed on the same day for the estimation of GSH-PX (catalog no. A005), total SOD (catalog no. A001-1), catalase (catalog no. A007-1), and T-AOC (catalog no. A015) by quantitative analysis using commercial reagent kits (Nanjing Jiancheng Bioengineering Institute, Nanjing, China) according to the manufacturer's instructions.

**2.9. Antioxidant and Antiapoptotic Effect of PDDP on 6-OHDA Induced Cytotoxicity toward SH-SY5Y Cells.** *2.9.1. Cell Culture and Treatment.* SH-SY5Y cells were seeded in 96-well culture plates ($4 \times 10^4$ cells/well) for viability assays or 6-well culture plates ($5 \times 10^5$ cells/well) for ROS, MMP, and cell apoptosis tests. On the next day, different treatments were given to the cells as shown in Table 1. Briefly, cells were treated with different concentrations of L-DOPA, BPD, and PDDP for 2 h, after which 100 $\mu$M of 6-OHDA was added, and cells were incubated for another 24 h.

**Table 1. Treatments Given to Different Groups in the Antioxidant and Antiapoptotic Effect of PDDP on 6-OHDA-Induced Cytotoxicity Towards SH-SY5Y Cells**

| groups | treatments |
|---|---|
| control | none |
| model | treated with 6-OHDA only (100 $\mu$M) for 24 h |
| L-DOPA | pretreated with 10 $\mu$M L-DOPA for 2 h before the addition of 6-OHDA (100 $\mu$M) |
| BPD | pretreated with 10 $\mu$M BPD for 2 h before the addition of 6-OHDA (100 $\mu$M) |
| PDDP2 | pretreated with 2.0 $\mu$M PDDP for 2 h before the addition of 6-OHDA (100 $\mu$M) |
| PDDP5 | pretreated with 5.0 $\mu$M PDDP for 2 h before the addition of 6-OHDA (100 $\mu$M) |
| PDDD10 | pretreated with 10 $\mu$M PDDP for 2 h before the addition of 6-OHDA (100 $\mu$M) |

*2.9.2. Cell Viability Assay.* Cell viability was measured using MTT reduction assay as described previously.[18] At the end of each treatment, MTT was added to the wells at a final concentration of 0.5 mg/mL, and cells were further incubated at 37 °C for 4 h. The insoluble formazan was dissolved in DMSO, and the determination was measured at 570 nm by a plate reader (Thermo, Varioskan Flash).

*2.9.3. ROS Measurement and Mitochondrial Membrane Potential (MMP) Determination.* Intracellular ROS was quantified using a commercial kit (catalog no. S0033, Beyotime, Jiangsu, China) following the manufacturer's instructions. Mitochondrial membrane potential was measured using the fluorescent dye JC-1 (Molecular Probes) according to the manufacturer's instructions of a commercial kit (catalog no. C2006, Beyotime, Jiangsu, China).

*2.9.4. Cell Apoptosis Assay.* The quantitative analysis of apoptosis induced by different treatment groups was performed by Annexin V-FITC/PI double staining using the Cell Apoptotic analysis kit (Beyotime, Jiangsu, China). Briefly, SH-SY5Y cells were seeded in 6-well culture plates and treated with 10 $\mu$M L-DOPA, BPD, and PDDP followed by 6-OHDA as described for the cell viability assays. At the end of the treatment, cells were harvested, washed with cold PBS, suspended in 0.5 mL binding buffer and stained by 5 $\mu$L Annexin V-FITC and 5 $\mu$L PI. The cells were incubated in the dark for 15 min and measured by Cytomics FC500 flow cytometer (Beckman Coulter, U.S.A.).

**2.10. Statistical Analysis.** Statistical comparisons were performed by one-way ANOVA for multiple groups, $p < 0.05$ and $p < 0.01$ were considered indications of statistical differences and statistically significantly different, respectively.

## 3. RESULTS

**3.1. Synthesis of *N*-3,4-Bis(pivaloyloxy)dopamine-3-(dimethylamino)propanamide (PDDP).** BPD, PDDP and DDP were synthesized as described in Scheme 1 and Scheme S1 in the SI. The structures of the conjugates were confirmed by electrospray ionization mass spectrometry (ESI-MS) and nuclear magnetic resonance ($^1$H NMR and $^{13}$C NMR).

The stability of BPD and PDDP was tested by incubating with rat plasma and brain homogenate and phosphate buffer solutions (pH 7.4). After 8 h incubation at 37 °C, 80% of the original amount of BPD (Figure 1a) and PDDP (Figure 1b) remained in the buffer, while <50% remained in plasma after 5 min incubation. A sustained release of PDDP was found in the brain with ∼30% remaining after 1 h incubation, which indicated a reasonable stability of PDDP. As reported previously,[20] dipivaloyloxy derivatives (BPD and PDDP) under-

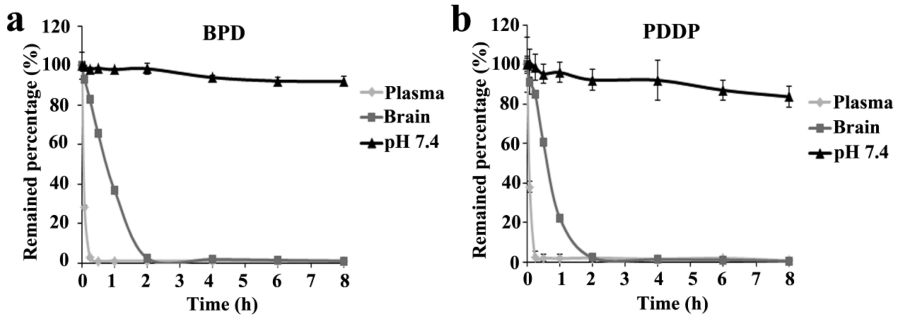


**Figure 1.** Stability of BPD (a) and PDDP (b) in plasma, brain homogenates, and 0.1 M PBS (pH = 7.4) at 37 °C for 8 h. Data represent mean ± SD ($n$ = 3).


dx.doi.org/10.1021/mp500352p | Mol. Pharmaceutics 2014, 11, 3174−3185

**Scheme 2. Enzymatic Hydrolysis of BPD and PDDP in Physiological Environment**

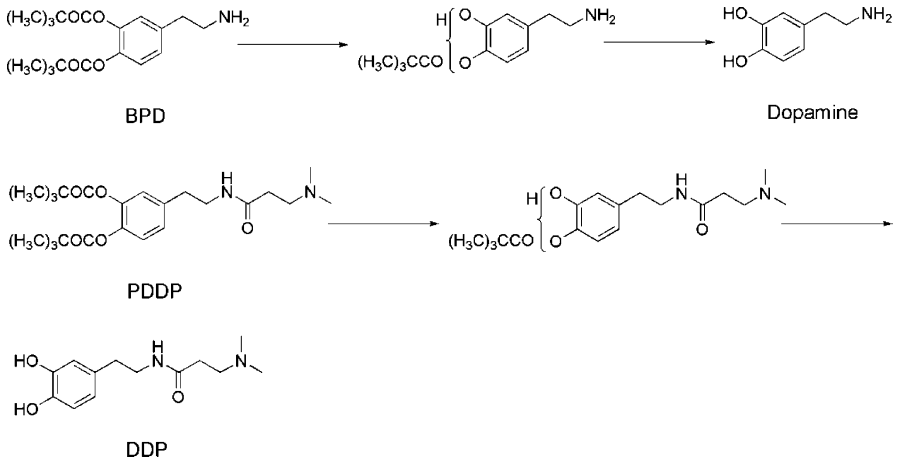


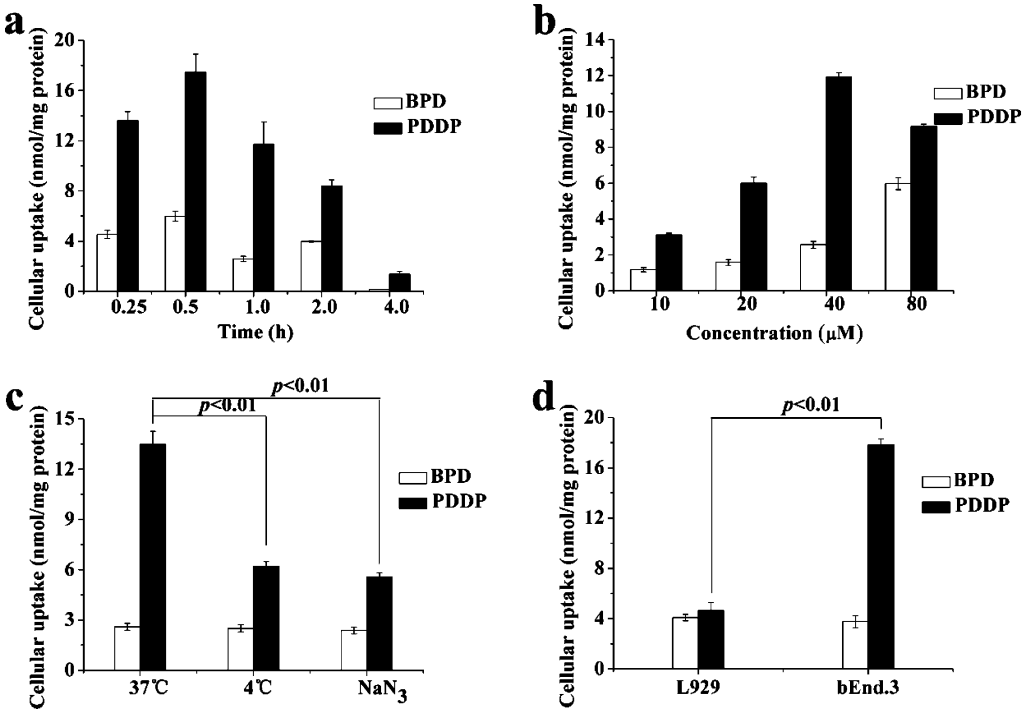


**Figure 2.** Cellular uptake of L-DOPA, BPD, and PDDP under various conditions; the intracellular concentration of L-DOPA was below the limit of detection in all cell uptake assays. Data represent mean ± SD ($n$ = 3): (a) Cellular uptake of BPD and PDDP (40 $\mu$M) in bEnd.3 cells at 0.25, 0.5, 1, 2, and 4 h. PDDP showed significantly higher uptake than BPD at all the time points examined. (b) Cellular uptake of BPD and PDDP in bEnd.3 cells at different doses (10, 20, 40, and 80 $\mu$M) at 37 °C for 0.5 h. PDDP showed higher uptake at all the doses examined. (c) Cellular uptake of BPD and PDDP (40 $\mu$M) in bEnd.3 cells at 37 °C, 4 °C, and in the presence of $NaN_3$ for 0.5 h. PDDP displayed a significantly higher uptake at 37 °C than at 4 °C and in the presence of $NaN_3$. (d) Comparison of the cellular uptake of BPD and PDDP (40 $\mu$M) in L929 cells and bEnd.3 cells at 37 °C for 0.5 h. L929 showed lower uptake of both BPD and PDDP, while in bEnd.3, the uptake of PDDP was about 5 times higher than that of BPD.

went a two-step hydrolysis. Scheme 2 shows the enzymatic hydrolysis process of BPD and PDDP in physiological environment.

**3.2. Cellular Uptake of PDDP in bEnd.3 Cells.** The uptake of PDDP by bEnd.3 cells was time-, concentration-, and temperature-dependent (Figure 2), indicating an active transport process. The uptake of PDDP by bEnd.3 cells was higher than the uptake of BPD during the 4 h incubation period (Figure 2a). At 0.5 h, the intracellular concentration of PDDP was saturated, and reached 17.47 ± 1.42 nmol/mg protein, which was 3.2-fold that of BPD (5.46 ± 0.38 nmol/mg). Figure 2b shows that cellular uptake in the PDDP group was significantly increased at different given doses compared with that in the BPD group. The intracellular concentration of PDDP was 4.6 times higher than that of BPD at the dose of 40 $\mu$M.

The uptake amount of PDDP at 37 °C (13.48 ± 0.78 nmol/mg) was much higher than that at 4 °C (6.19 ± 0.28 nmol/mg) and in the presence of $NaN_3$ (5.56 ± 0.24 nmol/mg), which indicated the potential dependence on temperature and energy. In contrast, the cellular uptake of BPD showed no substantial differences between 37 and 4 °C or in the presence of $NaN_3$ (Figure 2c). In Figure 2d, the cellular uptake of PDDP in bEnd.3 cells was much more than that in L929 cells,


dx.doi.org/10.1021/mp500352p | Mol. Pharmaceutics 2014, 11, 3174−3185

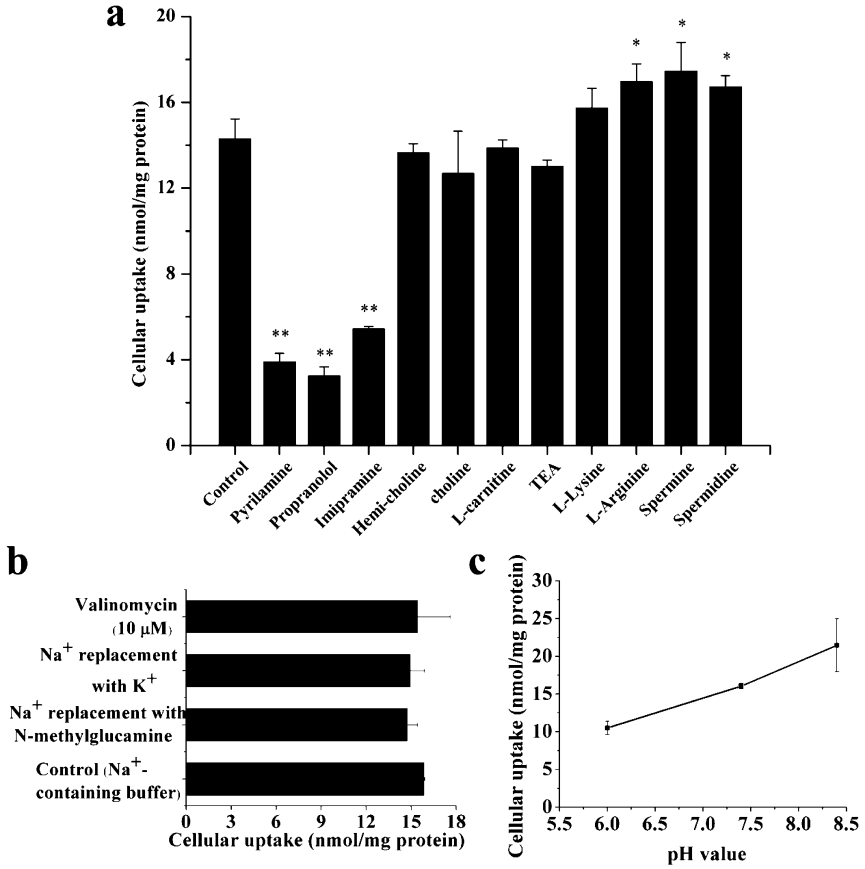


**Figure 3.** Mechanistic study on the brain-specific uptake of PDDP in vitro. Data represent mean ± SD ($n$ = 3): (a) Competitive inhibition of cellular uptake of PDDP (40 $\mu$M) by different inhibitors (pyrilamine, propranolol, imipramine, hemicholinium-3, choline, L-carnitine, TEA, L-lysine, L-arginine, spermine, and spermidine) at 37 °C for 0.5 h. Cationic drugs including pyrilamine, propranolol, and imipramine resulted in significantly reduced uptake of PDDP. *$p$ < 0.05, **$p$ < 0.01. (b) Effects of sodium ion replacement and membrane potential on PDDP uptake in bEnd.3 cells. Uptake of PDDP (40 $\mu$M) was measured at 37 °C for 0.5 h in sodium-containing (control) or sodium-free (replaced with *N*-methylglucamine or potassium) buffer. After pretreatment with valinomycin (10 $\mu$M), the uptake was measured in the sodium-containing buffer with valinomycin. (c) Effect of extracellular pH on PDDP (40 $\mu$M) uptake in bEnd.3 cells at 37 °C for 0.5 h.

demonstrating the cell selectivity of PDDP *in vitro*. However, no significant differences were observed for BPD between bEnd.3 and L929 cells. Moreover, the intracellular concentration of L-DOPA was below the limit of detection in all cellular uptake assays.

**3.3. Mechanistic Study on the Brain-Specific Uptake of PDDP *in Vitro*.** PDDP was proven to improve the cellular uptake efficacy in bEnd.3 cells by an active transport process. However, the mechanism behind it remains to be further addressed. Various transporter inhibitors were thus selected and incubated with PDDP, and their effects on the uptake were evaluated by the relative uptake efficiency (Figure 3a and Table S1 in the SI). The uptake was significantly inhibited by cationic inhibitors such as pyrilamine, propranolol, and imipramine, but not by hemicholinium-3 and choline (substrates or inhibitors of the choline transport system), L-carnitine (an OCTN2-specific substrate) and tetraethylammonium (classic inhibitor of OCTs). Alkaline amino acids such as L-lysine, L-arginine, spermine, and spermidine were shown to increase the cellular uptake of PDDP to some extent.

Figure 3b shows that the uptake of PDDP was not affected by the replacement of extracellular $Na^+$ with *N*-methylglucamine$^+$ or $K^+$. Treatment with valinomycin, a potassium ionopore, did not change the uptake of PDDP by bEnd.3 cells. pH dependence of the uptake of PDDP is shown in Figure 3c. The uptake was decreased by 40% in acidic transport medium (pH 6.0) and increased by 30% in alkaline medium (pH 8.4).

**3.4. Tissue Distribution and Brain Bioavailability of PDDP in Rats.** To further evaluate the brain targetability of PDDP, tissue distributions of L-DOPA, BPD, and PDDP were studied in rats. The brain drug concentration showed that the concentration of PDDP was significantly higher than those of L-DOPA and BPD throughout the time course (Figure 4a). Specifically, the PDDP concentration in brain was about 6.90 times higher than that of the BPD group at 5 min after *i.v.* injection in rats. As shown in Figure 4b, at 5 min, a higher distribution of PDDP was also observed in other tissues, which is 3.55 times more than that of BPD in heart, 3.69 times more in liver, 0.44 times more in lung, and 1.5 times more in kidney. BPD showed a similar distribution property with PDDP in the systemic circulation except in the brain, which indicated poor tissue-specific localization. In addition, L-DOPA was found to accumulate mainly in the kidney due to its short half-life *in vivo*.

In Figure 4c, the brain drug concentration in the PDDP group was significantly improved compared with that of L-DOPA and BPD groups at different time points. Table 2 indicates that the area under the curve ($AUC_{0-t}$) of PDDP was 116.35 times and 4.63 times higher than that of L-DOPA and BPD, respectively. The maximal concentration ($C_{max}$) was


dx.doi.org/10.1021/mp500352p | *Mol. Pharmaceutics* 2014, 11, 3174−3185

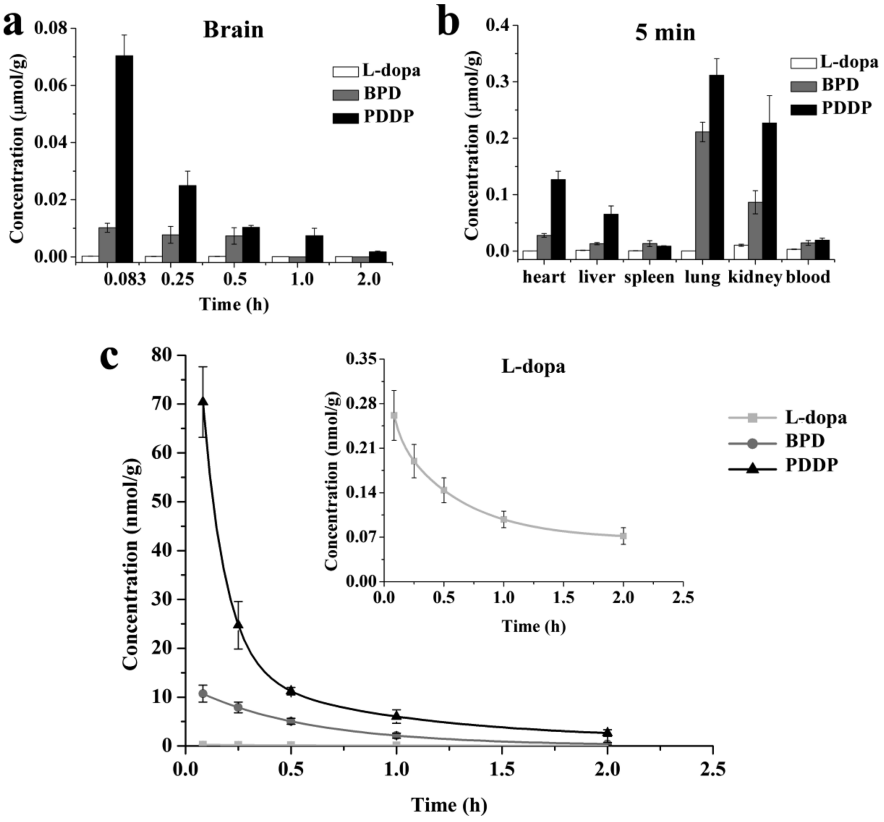


**Figure 4.** Biodistribution in rats after *i.v.* injection of L-DOPA, BPD, and PDDP. Data represent mean ± SD ($n$ = 5). (a) Levels of L-dopa, BPD, and PDDP in brain. (b) Drug levels in other tissues (heart, liver, spleen, lung, kidney, and plasma) at 5 min. PDDP is selectively concentrated in lung, kidney, and brain, especially in the brain. At 5 min, in brain the concentration of PDDP is ∼7 times that of the BPD concentration. (c) Brain bioavailability in rats after *i.v.* injection of L-DOPA, BPD, and PDDP. PDDP displayed significantly higher concentrations than L-DOPA and BPD during the entire course of the investigation.

**Table 2. Pharmacokinetic Parameters of L-DOPA, BPD, and PDDP in Brain after *i.v.* Injection in Rats**

| parameters | L-DOPA | BPD | PDDP |
|---|---|---|---|
| $AUC_{0\text{-}t,brain}$ (nmol/g*h) | 0.24 ± 0.013 | 6.07 ± 0.73 | 28.14 ± 1.35 |
| $C_{max,brain}$ (nmol/g) | 0.26 ± 0.039 | 10.98 ± 1.26 | 70.39 ± 7.24 |
| $Re_{brain}$ | – | 25.11 | 116.35 |
| $Ce_{brain}$ | – | 42.00 | 269.28 |

269.28 times and 6.41 times higher than that of L-DOPA and BPD, respectively. The above results demonstrate the bioavailability improvement of PDDP in the brain.

**3.5. Therapeutic Effect of PDDP on 6-OHDA-Induced PD Model in Rat.** To explore the utility of PDDP in the treatment of PD, PDDP was injected to the 6-OHDA-lesioned model rats. The striatal dopamine contents and striatal tyrosine hydroxylase (TH) immunohistochemistry were used to evaluate the therapeutic effects of PDDP. On day 21, the amount of dopamine in the lesioned striatum after different

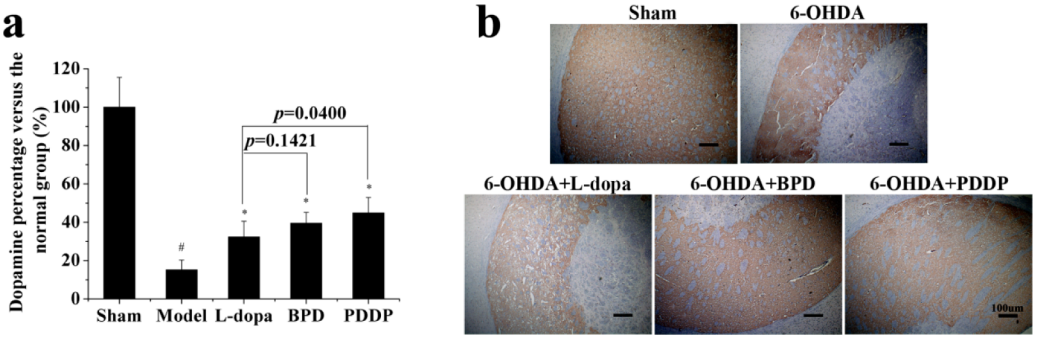


**Figure 5.** Therapeutic effect of L-DOPA, BPD, and PDDP on 6-OHDA rat model of Parkinson's disease. Data represent mean ± SD $^{\#}p < 0.01$ with respect to the sham group, $^{*}p < 0.01$ with respect to the 6-OHDA lesioned group. (a) Dopamine percentage in the 6-OHDA lesioned striatum of rats 3 weeks after 6-OHDA lesion ($n$ = 5). (b) TH-immunoreactivity in the striatum of rats of different groups 3 weeks after 6-OHDA lesion. Scale bar: 100 μm. After PDDP administration, a significant increase was observed in dopamine content and TH-immunopositive neurons (brown staining), while L-DOPA- and BPD-treated groups showed certain but weaker therapeutic effects.


dx.doi.org/10.1021/mp500352p | *Mol. Pharmaceutics* 2014, 11, 3174−3185

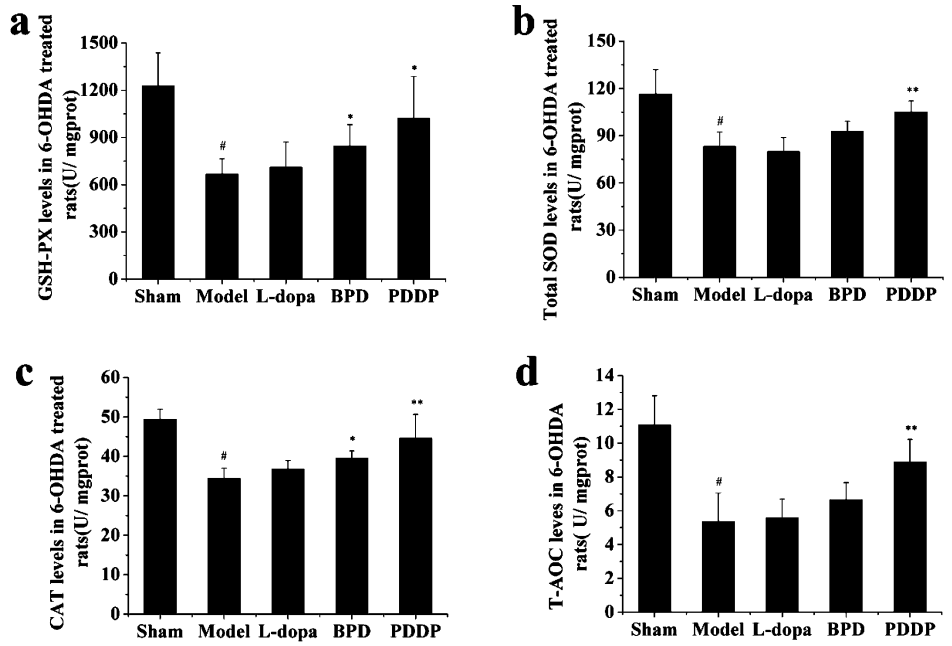


**Figure 6.** Oxidative stress in ipsilateral striatum of different treatment groups in the 6-OHDA rat model of PD. Data represent mean ± SD ($n$ = 5). $^{\#}p < 0.01$ vs the sham group, $^{*}p < 0.05$ and $^{**}p < 0.01$ vs the 6-OHDA lesioned group. (a) GSH-PX, (b) total SOD, (c) catalase, and (d) total antioxidant capacity (T-AOC). PDDP-treated group showed a remarkable increase in antioxidant enzymes compared with the model group.

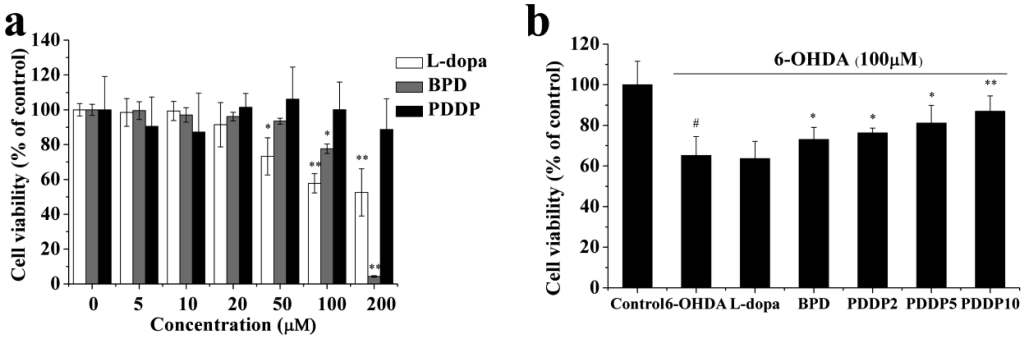


**Figure 7.** Protective effect of PDDP against cell injury induced by 6-OHDA in SH-SY5Y cells. (a) The cell viability of SH-SY5Y cells treated by L-DOPA, BPD, and PDDP at concentrations of 0, 5, 10, 20, 50, 100, and 200 $\mu$M. After 24 h, the cell viability was determined by MTT assay ($n$ = 3). L-dOpa and BPD induced severe cytotoxicity in SH-SY5Y cells when the concentration reached 50 $\mu$M. $^{*}p < 0.05$ and $^{**}p < 0.01$ versus untreated cells. (b) The effects of L-DOPA, BPD, and PDDP on the cell viability of 6-OHDA-treated (100 $\mu$M) SH-SY5Y cells. Cells were pretreated with L-DOPA (10 $\mu$M), BPD (10 $\mu$M), and different concentrations of PDDP (2.0, 5.0, and 10 $\mu$M) for 2 h before the addition of 6-OHDA. The results showed PDDP increased the cell viability in a dose-dependent manner. Data represent mean ± SD ($n$ = 3). $^{\#}p < 0.01$ vs untreated cells, $^{*}p < 0.05$ and $^{**}p < 0.01$ vs 6-OHDA-treated group.

treatments is shown in Figure 5a. The amount of DA in 6-OHDA-lesioned group decreased to 15.22% compared to the sham group, which demonstrated the successful establishment of the 6-OHDA model. After treatment with L-DOPA and conjugates, the amount of DA increased at various degrees compared with the 6-OHDA group, while PDDP treatment (44.85%) showed a much higher increase in DA than L-DOPA (32.32%) and BPD (39.51%) treatment.

Brain sections of rats after different treatments were performed for the TH-immunohistochemistry on day 21. The sham group did not show any loss in TH-immunohistochemistry in the striatum of the infusion side (Figure 5b). However, in the 6-OHDA group, the striatum region infused with 6-OHDA showed extensive lesion as evidenced by significantly lesser TH-immunoreactive neurons compared to the sham group. After PDDP administration, there was a remarkable improvement in the TH-immunopositive neurons in the 6-OHDA-infused side, while L-DOPA- and BPD-treated groups showed certain but weaker therapeutic effects.

Long-term usage of L-DOPA could accelerate the neuron degeneration resulting from oxidative stress. Thus, we studied the oxidative stress level in the striatum after treatment with PDDP. The results are summarized in Figure 6. A significant decrease ($p < 0.001$) in GSH-PX, T-SOD, CAT, and T-AOC was observed in striatum of 6-OHDA-lesioned group when compared to that of the sham group, which was remarkably restored by 28.92%, 18.80%, 20.65%, and 31.74%, respectively, in the PDDP treatment group as compared to the model rats. The BPD treatment group exhibited significant increases in striatal GSH-PX and CAT by 14.62% and 10.35%, respectively, compared to the 6-OHDA-lesioned group. However, the L-DOPA-treated group showed no obvious change in antioxidant enzyme activities compared with that of the lesioned rats.


dx.doi.org/10.1021/mp500352p | Mol. Pharmaceutics 2014, 11, 3174−3185

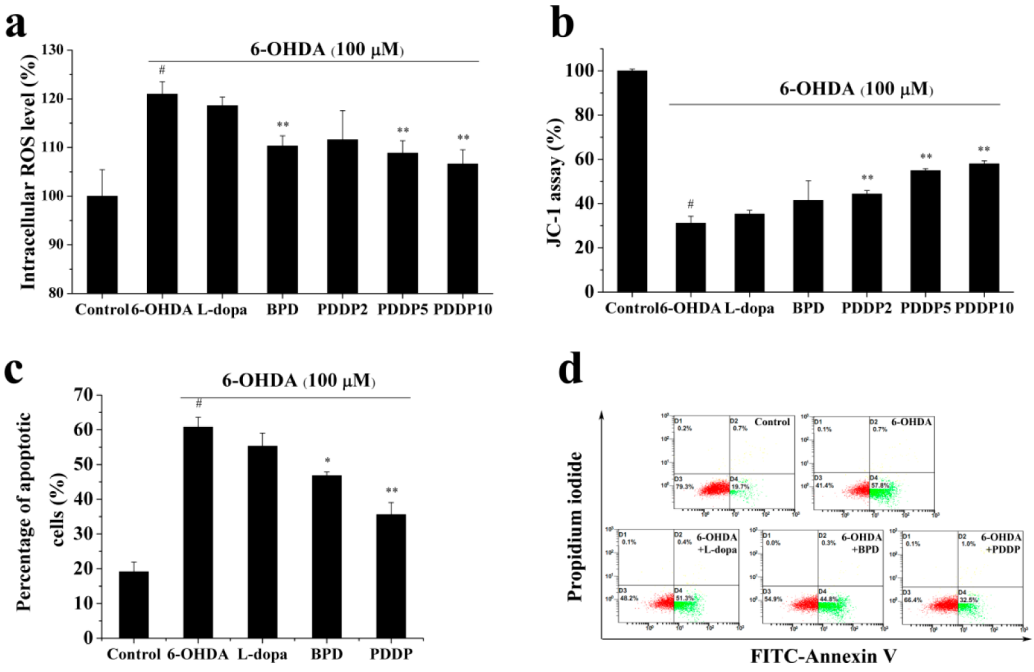


**Figure 8.** Effect of PDDP on oxidative stress and cell apoptosis induced by 6-OHDA in SH-SY5Y cells. Cells were treated with no 6-OHDA (control) or with 100 $\mu$M 6-OHDA after pretreatment with L-DOPA (10 $\mu$M), BPD (10 $\mu$M), and different concentrations of PDDP (2.0, 5.0, and 10 $\mu$M). Results were normalized to the percentage of control. Data represent mean ± SD, $n = 3$. $^{\#}p < 0.01$ with respect to the untreated cells, $^{*}p < 0.05$ and $^{**}p < 0.01$ with respect to the 6-OHDA-treated group. (a) Levels of ROS were measured using the DCFH-DA assay; (b) mitochondrial membrane potential (MMP) was measured using JC-1 staining; (c) proportion of apoptotic cells after different treatments; (d) apoptosis assays conducted by flow cytometry using annexin V in combination with propidium iodide. The obtained results suggested that PDDP could inhibit oxidative stress and neuronal apoptosis induced by 6-OHDA.

**Scheme 3. Neuroprotection of PDDP in 6-OHDA-Induced SH-SY5Y Cells**

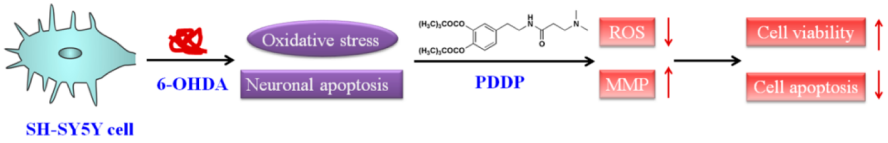


### 3.6. Antioxidant and Antiapoptoptic Effect of PDDP on 6-OHDA-Induced Cytotoxicity toward SH-SY5Y Cells.

L-DOPA-induced neurotoxicity is thought to be involved in the side effects of L-DOPA therapy. In this study, we try to substantiate whether PDDP could induce cytotoxicity to neurons as L-DOPA did. Catecholaminergic neuroblatoma SH-SY5Y cells were employed to assess the effects. L-DOPA could induce cytotoxicity in SH-SY5Y cells when the concentration reached 50 $\mu$M (Figure 7a), whereas PDDP did not induce any cytotoxicity with the same doses. To further evaluate the protective effect of PDDP against 6-OHDA-induced cell injury in SH-SY5Y cells, cells were pretreated with PDDP at different concentrations for 2 h before addition of 6-OHDA (100 $\mu$M) for another 24 h. As shown in Figure 7b, treating SH-SY5Y cells with 100 $\mu$M 6-OHDA reduced the cell viability to 65% of the control, while PDDP increased cell viability in a dose-dependent manner: 2.0 $\mu$M, 76.30%; 5.0 $\mu$M, 81.09%; and 10 $\mu$M, 86.92% of the control, respectively. Whereas, neither L-DOPA nor BPD at the equal molar concentration (10 $\mu$M) was sufficient to exert the similar protective effects against 6-OHDA-induced cell injury as PDDP did.

6-OHDA is known to selectively kill dopaminergic neurons by generating reactive oxygen species (ROS) and inducing oxidative stress in the cells. We thus proceeded to examine the effect of PDDP on 6-OHDA-induced ROS formation in SH-SY5Y cells. Figure 8a shows that exposing cells to 100 $\mu$M 6-OHDA for 24 h increased ROS to 120.99% of control value. Pretreating cells with different concentrations of PDDP for 2 h ameliorated the 6-OHDA-induced ROS formation in a dose-dependent manner. In comparison, BPD suppressed the 6-OHDA-induced ROS formation to a much lesser extent. Mitochondrial membrane potential (MMP) is essential for cell survival, particularly cells that are under oxidative stress. Treating cells with 100 $\mu$M 6-OHDA for 24 h decreased MMP to 31.13% of control value based on JC-1 assay (Figure 8b). Pretreating cells with different concentrations of PDDP for 2 h ameliorated the 6-OHDA-induced MMP reduction in a dose-dependent manner.

The effects of PDDP pretreatment on 6-OHDA-induced apoptosis were analyzed by double staining with FITC annexin-V and propidium iodide. Cells showing FITC-positivity only were considered to be in an early apoptotic phase. According to Figure 8c, exposing SH-SY5Y cells to 6-OHDA significantly increased the level of apoptosis (with apoptotic rate of 60.77 ± 2.83%) than in the absence of 6-OHDA (with apoptotic rate of 19.13 ± 2.80%); however, this increase was attenuated by pretreatment with 10 $\mu$M PDDP (with apoptotic rate of 35.37 ± 3.46%). Therefore, PDDP was shown to protect SH-SY5Y


dx.doi.org/10.1021/mp500352p | Mol. Pharmaceutics 2014, 11, 3174−3185

cells from 6-OHDA-induced cell apoptosis and improve cell viability (Scheme 3).

## 4. DISCUSSION

PD is an age-related progressive degenerative disease with motor disorders such as bradykinesia, resting tremor, rigidity, and postural instability.[2] To date, L-DOPA treatment remains the most effective therapy for PD which compensates for the dopamine deficiency. However, L-DOPA cannot arrest the progression of PD, and the long-term application of L-DOPA induces dyskinesia and accelerates the neuron degeneration.[21] Thus, a delivery system with better therapeutic effects and reduced side effects is highly demanded for the treatment of PD.

In previous works, our group has shown that *N*,*N*-dimethylethylenediamine-related structures significantly enhanced the targeting efficiency of naproxen and dexibuprofen to the brain.[15,16] The ligand offers many advantages such as a well-defined structure, minimum cytotoxicity, and high efficiency of brain targeting. Thus, we designed and synthesized DDP, which is the conjugate of dopamine and *N*,*N*-dimethylamino propanoic acid to improve the brain targetability. However, DDP was proven not a qualified candidate for brain targeting, which did not show brain-specific accumulation after systemic administration (data not shown). After careful examination, lipophilicity appeared to be an important impact factor for achieving brain targeting. Therefore, the dipivaloyloxy functional group was introduced in the synthesis of *N*-3,4-bis(pivaloyloxy)dopamine-3-(dimethylamino)propanamide (PDDP) to increase the overall lipophilicity of the conjugate, thus improving brain targetability. To our best knowledge, no published reports are available regarding *N*,*N*-dimethyl amino group as a brain-targeted ligand. Also, this is the first report to confirm the essential role of lipophilicity for *N*,*N*-dimethyl amino group-conjugated drug derivatives to achieve brain targeting. In this regard, the substrates of the novel brain-targeting ligand would be largely extended. More importantly, the *N*,*N*-dimethyl amino group offers an alternative approach to the brain-specific delivery of therapeutic agents for central nervous system diseases.

Previous research confirmed the brain targetability of *N*,*N*-dimethylethylenediamine-related structures by studying the biodistribution of the conjugate in animals, which did not explore the mechanism of the improved brain accumulation, especially the transport process across the BBB. In this study, the bEnd.3 cell-based BBB model was chosen and established to study the brain delivery of the conjugate. Enhanced intracellular delivery of PDDP was observed in bEnd.3 cells, which was significantly higher than that of L-DOPA and BPD. Mechanistic investigation further revealed that PDDP entering bEnd.3 cells required energy which probably occurred through an active transport process (Figure 2). On the contrary, BPD did not require energy and showed poor uptake efficiency in both bEnd.3 cells and L929 cells, which suggested a passive diffusion process. In addition, DDP could not be uptaken by either bEnd.3 or L929 cells. Thus, both *N*,*N*-dimethyl amino and dipivaloyloxy groups are essential structures in the PDDP for transport across the BBB, which confirmed our previous hypothesis.

To reveal the driving force behind the specific transport, a competitive inhibition assay was conducted in bEnd.3 cells. Cationic compounds, choline and analogs, did not inhibit the uptake of PDDP, nor did alkaline amino acids (Figure 3a). Thus, PDDP uptake was not triggered by organic cationic transporters, choline transporters, or the electrostatic interactions as observed in the transport of cationic peptides.[22] This conclusion was supported by the membrane potential independence (Figure 3b) and pH dependence (Figure 3c) of PDDP uptake in bEnd.3 cells. In contrast, the lipophilic cationic drugs pyrilamine, imipramine, and propranolol significantly inhibited the uptake of PDDP in bEnd.3 cells. Yamazaki et al.[23,24] demonstrated that pyrilamine and other basic lipophilic agents[25−27] were transferred into the brain by an organic cation-sensitive transport system, i.e., putative pyrilamine transporters. Competitive inhibition of these agents on PDDP uptake indicated that putative pyrilamine cationic transporters were involved in the brain uptake of PDDP, which remained to be elucidated at the molecular level.

*In vitro* stability is an important prediction of the *in vivo* fate for drug conjugates. As previously reported,[20] dipivaloyloxy derivatives were suggested to undergo a two-step enzymatic hydrolysis process (Scheme 2). PDDP showed a prolonged release in the brain homogenates, which would likely result in a sustained therapeutic effect. On the basis of these results, we proposed the following physiological disposition process for brain delivery of PDDP: after systemic injection, PDDP may undergo a rapid distribution to tissues due to its high lipophilicity, which was attributed to the dipivaloyloxy structure; meanwhile, with the conjugation of the *N*,*N*-dimethylamino group, PDDP can be specifically recognized by transporters expressed in the brain microvascular endothelial cells and then be transported into the brain. Moreover, the relative lower pH in the brain (intracellular pH $\approx$ 7.0) than blood circulation (pH $\approx$ 7.4)[28,29] may induce the ionization of tertiary amines in the derivative, which may help PDDP to be retained in the brain, thereby resulting in significantly higher brain specificity as demonstrated in biodistribution and brain bioavailability study (Figure 4).

In addition to its selective transport across the BBB and the rapid accumulation in the brain tissue, PDDP is readily hydrolyzed to DDP by ubiquitous esterases in brain. The generation of DDP is a prolonged and continuous process as discussed above. The primary amine of dopamine is not an essential requirement for dopaminergic activity,[30] and thus, PDDP may retain the intrinsic activity of dopamine without the cleavage of the amide bond in PDDP. As a result, effective therapeutic performance of PDDP was observed in 6-OHDA-lesioned PD rats. Our data showed that PDDP could effectively attenuate the striatum lesion induced by 6-OHDA, while L-DOPA and BPD treatment showed certain but weaker therapeutic effects (Figure 5). Recent studies revealed that oxidative stress plays an important role in the neurodegenerative pathogenesis of PD.[31] Dopamine and L-DOPA were found to increase oxidative stress and thus aggravate the condition of PD patients.[32] Novel therapeutic strategies have been developed using neuroprotective agents in the management of PD. Here, PDDP was proven effective to increase the level of antioxidant enzymes including GSH-PX, total SOD, catalase, and T-AOC (Figure 6). Thus, the suppression of oxidative injury is likely the primary mechanism for the protective effect of PDDP in the unilateral 6-OHDA PD rat model.

Dopamine- and L-DOPA-induced neurotoxicity is thought to be involved in the side effects of L-DOPA therapy.[33] DA and its metabolites containing two hydroxyl residues were reported to display dose-dependent cytotoxicity in dopaminergic neuronal

cells mainly due to the generation of highly reactive DA and DOPA quinones which are dopaminergic neuron-specific cytotoxic molecules.[34] The two hydroxyl groups in PDDP were protected by dipivaloyloxy, and PDDP displayed a slow and continuous release in the brain. In consequence, PDDP was less likely to generate quinone radicals in the brain. In the cytotoxicity study, L-DOPA showed dose-dependent damages to catecholaminergic neuroblatoma SH-SY5Y cells in accord with previous studies,[35] while PDDP did not induce cytotoxicity at the same doses (Figure 7a). Interestingly, PDDP increased the viability of cells treated by 6-OHDA in a dose-dependent manner. Furthermore, PDDP showed the ability to suppress the 6-OHDA-induced ROS formation and increase 6-OHDA-induced MMP reduction, as well as inhibit neuronal apoptosis induced by 6-OHDA (Figure 8). Therefore, we conclude that PDDP could present neuroprotective effect in 6-OHDA-induced SH-SY5Y cells.

PDDP was demonstrated to be selectively delivered to the brain with improved therapeutic efficacy and reduced side effects. The study also showed that PDDP displayed good biocompatibility and safety through *in vitro* and *in vivo* evaluation (Figure S1 in SI). Future studies should focus on the thorough understanding of the enhanced uptake and improved efficacy of PDDP.

## 5. CONCLUSION

In summary, a brain-specific derivative of dopamine (PDDP) was developed by lipophilic modification with dipivaloyloxy and conjugation with *N*,*N*-dimethylamino propanoic acid, which presented a promising small molecular conjugate with improved brain targetability. The uptake of PDDP in bEnd.3 cells could be inhibited by lipophilic cationic drugs, indicating putative pyrilamine cationic transporters might be involved in the uptake of PDDP. Moreover, the derivative showed excellent brain targeting properties and superior therapeutic effects in the 6-OHDA-lesioned rat model. The antioxidant and antiapoptotic effect of PDDP appeared to protect SH-SY5Y cells from 6-OHDA-induced toxicity. Therefore, PDDP would be a promising drug candidate that can be applied for the targeted PD treatment. Additionally, conjugation of other lipophilic therapeutics to the *N*,*N*-dimethyl amino group may offer alternative treatments for CNS diseases.

## ■ ASSOCIATED CONTENT

### Supporting Information

Additional experimental details and figures including the synthetic methods and structure confirmation. This material is available free of charge via the Internet at http://pubs.acs.org.

## ■ AUTHOR INFORMATION

### Corresponding Author

*Telephone: +86-28-85501566. Fax: +86-28-85501615. E-mail: zrzzl@vip.sina.com.

### Notes

The authors declare no competing financial interest.

## ■ ACKNOWLEDGMENTS

We are grateful for the financial support from the National Science Foundation of China (No. 81130060) and the National Basic Research Program of China (No. 2013CB932504).

## ■ ABBREVIATIONS:

PD, Parkinson's disease; DA, dopamine; TH, tyrosine hydroxylase; BBB, blood brain barrier; CNS, central nervous system; PDDP, *N*-3,4-bis(pivaloyloxy)dopamine-3-(dimethylamino)propanamide; BPD, 3,4-bis (pivaloyloxy)-dopamine; DDP, *N*-(3,4-dihydroxyphenethyl)-3-(dimethylamino)propanamide

## ■ REFERENCES

(1) Serra, P. A.; Esposito, G.; Enrico, P.; Mura, M. A.; Migheli, R.; Delogu, M. R.; Miele, M.; Desole, M. S.; Grella, G.; Miele, E. Manganese increases L-DOPA auto-oxidation in the striatum of the freely moving rat: Potential implications to L-DOPA long-term therapy of Parkinson's disease. *Br. J. Pharmacol.* **2000**, *130* (4), 937–945.

(2) Olanow, C. W.; Schapira, A. H. Therapeutic prospects for Parkinson disease. *Ann. Neurol.* **2013**, *74* (3), 337–347.

(3) Kao, H. D.; Traboulsi, A.; Itoh, S.; Dittert, L.; Hussain, A. Enhancement of the systemic and CNS specific delivery of L-dopa by the nasal administration of its water soluble prodrugs. *Pharm. Res.* **2000**, *17* (8), 978–984.

(4) Olanow, C. W. Levodopa/dopamine replacement strategies in Parkinson's disease–Future directions. *Mov. Disord.* **2008**, *23* (Suppl 3), S613–S622.

(5) Ossig, C.; Reichmann, H. Treatment of Parkinson's disease in the advanced stage. *J. Neural Transm.* **2013**, *120* (4), 523–529.

(6) Zhou, T.; Hider, R. C.; Jenner, P.; Campbell, B.; Hobbs, C. J.; Rose, S.; Jairaj, M.; Tayarani-Binazir, K. A.; Syme, A. Design, synthesis and biological evaluation of peptide derivatives of L-dopa as anti-Parkinsonian agents. *Bioorg. Med. Chem. Lett.* **2013**, *23* (19), 5279–5282.

(7) Warren Olanow, C.; Kieburtz, K.; Rascol, O.; Poewe, W.; Schapira, A. H.; Emre, M.; Nissinen, H.; Leinonen, M.; Stocchi, F. Factors predictive of the development of Levodopa-induced dyskinesia and wearing-off in Parkinson's disease. *Mov. Disord.* **2013**, *28* (8), 1064–1071.

(8) Carelli, V.; Liberatore, F.; Scipione, L.; Impicciatore, M.; Barocelli, E.; Cardellini, M.; Giorgioni, G. New systems for the specific delivery and sustained release of dopamine to the brain. *J. Controlled Release* **1996**, *42* (3), 209–216.

(9) Denora, N.; Trapani, A.; Laquintana, V.; Lopedota, A.; Trapani, G. Recent advances in medicinal chemistry and pharmaceutical technology-strategies for drug delivery to the brain. *Curr. Top. Med. Chem.* **2009**, *9* (2), 182–196.

(10) Bonina, F.; Puglia, C.; Rimoli, M. G.; Melisi, D.; Boatto, G.; Nieddu, M.; Calignano, A.; Rana, G. L.; Caprariis, P. d. Glycosyl derivatives of dopamine and L-dopa as anti-Parkinson prodrugs: synthesis, pharmacological activity and in vitro stability studies. *J. Drug Target.* **2003**, *11* (1), 25–36.

(11) Fernández, C.; Nieto, O.; Rivas, E.; Montenegro, G.; Fontenla, J. A.; Fernández-Mayoralas, A. Synthesis and biological studies of glycosyl dopamine derivatives as potential antiparkinsonian agents. *Carbohydr. Res.* **2000**, *327* (4), 353–365.

(12) Dalpiaz, A.; Filosa, R.; de Caprariis, P.; Conte, G.; Bortolotti, F.; Biondi, C.; Scatturin, A.; Prasad, P. D.; Pavan, B. Molecular mechanism involved in the transport of a prodrug dopamine glycosyl conjugate. *Int. J. Pharm.* **2007**, *336* (1), 133–139.

(13) Peura, L.; Malmioja, K.; Huttunen, K.; Leppänen, J.; Hämäläinen, M.; Forsberg, M. M.; Rautio, J.; Laine, K. Design, synthesis and brain uptake of LAT1-targeted amino acid prodrugs of dopamine. *Pharm. Res.* **2013**, *30* (10), 2523–2537.

(14) Denora, N.; Laquintana, V.; Lopedota, A.; Serra, M.; Dazzi, L.; Biggio, G.; Pal, D.; Mitra, A. K.; Latrofa, A.; Trapani, G.; Liso, G. Novel L-Dopa and dopamine prodrugs containing a 2-phenyl-imidazopyridine moiety. *Pharm. Res.* **2007**, *24* (7), 1309–1324.

(15) Zhang, X.; Liu, X.; Gong, T.; Sun, X.; Zhang, Z.-r. In vitro and in vivo investigation of dexibuprofen derivatives for CNS delivery. *Acta Pharmacol. Sin.* **2012**, *33* (2), 279–288.

(16) Zhang, Q.; Liang, Z.; Chen, L.; Sun, X.; Gong, T.; Zhang, Z. Novel brain targeting prodrugs of naproxen based on dimethylamino group with various linkages. *Arzneim.-Forsch.* **2012**, *62* (06), 261−266.
(17) Chemuturi, N. V.; Donovan, M. D. Role of organic cation transporters in dopamine uptake across olfactory and nasal respiratory tissues. *Mol. Pharmaceutics* **2007**, *4* (6), 936−942.
(18) Hu, K.; Shi, Y.; Jiang, W.; Han, J.; Huang, S.; Jiang, X. Lactoferrin conjugated PEG-PLGA nanoparticles for brain delivery: Preparation, characterization and efficacy in Parkinson's disease. *Int. J. Pharm.* **2011**, *415* (1−2), 273−283.
(19) Wen, Z.; Yan, Z.; Hu, K.; Pang, Z.; Cheng, X.; Guo, L.; Zhang, Q.; Jiang, X.; Fang, L.; Lai, R. Odorranalectin-conjugated nanoparticles: Preparation, brain delivery and pharmacodynamic study on Parkinson's disease following intranasal administration. *J. Controlled Release* **2011**, *151* (2), 131−138.
(20) Bodor, N.; Farag, H. H. Improved delivery through biological membranes. 13. Brain-specific delivery of dopamine with a dihydropyridine ⇌ pyridinium salt type redox delivery system. *J. Med. Chem.* **1983**, *26* (4), 528−534.
(21) Xie, L.; Hu, L.-F.; Teo, X. Q.; Tiong, C. X.; Tazzari, V.; Sparatore, A.; Del Soldato, P.; Dawe, G. S.; Bian, J.-S. Therapeutic effect of hydrogen sulfide-releasing L-Dopa derivative ACS84 on 6-OHDA-induced Parkinson's disease rat model. *PloS One* **2013**, *8* (4), e60200.
(22) Deguchi, Y.; Miyakawa, Y.; Sakurada, S.; Naito, Y.; Morimoto, K.; Ohtsuki, S.; Hosoya, K.-i.; Terasaki, T. Blood−brain barrier transport of a novel $\mu$1-specific opioid peptide, H-Tyr-d-Arg-Phe-$\beta$-Ala-OH (TAPA). *J. Neurochem.* **2003**, *84* (5), 1154−1161.
(23) Yamazaki, M.; Terasaki, T.; Yoshioka, K.; Nagata, O.; Kato, H.; Ito, Y.; Tsuji, A. Carrier-mediated transport of H1-antagonist at the blood-brain barrier: A common transport system of H1-antagonists and lipophilic basic drugs. *Pharm. Res.* **1994**, *11* (11), 1516−1518.
(24) Yamazaki, M.; Terasaki, T.; Yoshioka, K.; Nagata, O.; Kato, H.; Ito, Y.; Tsuji, A. Carrier-mediated transport of H1-antagonist at the blood-brain barrier: Mepyramine uptake into bovine brain capillary endothelial cells in primary monolayer cultures. *Pharm. Res.* **1994**, *11* (7), 975−978.
(25) Okura, T.; Ito, R.; Ishiguro, N.; Tamai, I.; Deguchi, Y. Blood-brain barrier transport of pramipexole, a dopamine D2 agonist. *Life Sci.* **2007**, *80* (17), 1564−1571.
(26) Okura, T.; Hattori, A.; Takano, Y.; Sato, T.; Hammarlund-Udenaes, M.; Terasaki, T.; Deguchi, Y. Involvement of the Pyrilamine Transporter, a Putative Organic Cation Transporter, in Blood-Brain Barrier Transport of Oxycodone. *Drug Metab. Dispos.* **2008**, *36* (10), 2005−2013.
(27) Pardridge, W. M.; Sakiyama, R.; Fierer, G. Transport of propranolol and lidocaine through the rat blood-brain barrier. Primary role of globulin-bound drug. *J. Clin. Invest.* **1983**, *71* (4), 900.
(28) Kung, H. F.; Blau, M. Regional intracellular pH shift: a proposed new mechanism for radiopharmaceutical uptake in brain and other tissues. *J. Nucl. Med.* **1980**, *21* (2), 147−152.
(29) Kung, H. F.; Tramposch, K. M.; Blau, M. A new brain perfusion imaging agent:[I-123] HIPDM: N,N,N′-trimethyl-N′-[2-hydroxy-3-methyl-5-iodobenzyl]-1,3-propanediamine. *J. Nucl. Med.* **1983**, *24* (1), 66−72.
(30) Borgman, R. J.; McPhillips, J. J.; Stitzel, R. E.; Goodman, I. J. Synthesis and pharmacology of centrally acting dopamine derivatives and analogs in relation to Parkinson's disease. *J. Med. Chem.* **1973**, *16* (6), 630−633.
(31) Shin, K. S.; Choi, H. S.; Zhao, T. T.; Suh, K. H.; Kwon, I. H.; Choi, S. O.; Lee, M. K. Neurotoxic effects of berberine on long-term L-DOPA administration in 6-hydroxydopamine-lesioned rat model of Parkinson's disease. *Arch. Pharm. Res.* **2013**, *36* (6), 759−67.
(32) Le, W.; Jankovic, J.; Xie, W.; Appel, S. Antioxidant property of pramipexole independent of dopamine receptor activation in neuroprotection. *J. Neural Transm.* **2000**, *107* (10), 1165−1173.
(33) Gómez-Santos, C.; Ferrer, I.; Santidrián, A. F.; Barrachina, M.; Gil, J.; Ambrosio, S. Dopamine induces autophagic cell death and $\alpha$-synuclein increase in human neuroblastoma SH-SY5Y cells. *J. Neurosci. Res.* **2003**, *73* (3), 341−350.
(34) Asanuma, M.; Miyazaki, I.; Ogawa, N. Dopamine-or L-DOPA-induced neurotoxicity: The role of dopamine quinone formation and tyrosinase in a model of Parkinson's disease. *Neurotox. Res.* **2003**, *5* (3), 165−176.
(35) Lai, C.-T.; Yu, P. H. Dopamine-and L-$\beta$-3,4-dihydroxyphenylalanine hydrochloride (L-DOPA)-induced cytotoxicity towards catecholaminergic neuroblastoma SH-SY5Y cells: Effects of oxidative stress and antioxidative factors. *Biochem. Pharmacol.* **1997**, *53* (3), 363−372.